Manuscript refereed by Dr Karin Frisk (Swerea KIMAB, Sweden)

Influence of the Diamond Size and Diamond Distribution on the Wear Behaviour of Sintered Diamond-Metal Composites during the Machining of Reinforced Concrete - Investigations by Computer Tomography and Statistical Evaluations

W. Tillmann (Institute of Materials Engineering – TU Dortmund, Leonhard-Euler-Str. 2, 44227 Dortmund, Germany) wolfgang.tillmann@udo.edu; D. Biermann (Institute of Machining Technology, TU Dortmund, Baroper Straße 303, 44227 Dortmund,Germany) biermann@isf.de; C. Weihs (Chair of Computational Statistics, TU-Dortmund, Technische Universität Dortmund - 44221 Dortmund, Germany) weihs@statistik.uni-dortmund.de; M. Ferreira (Institute of Materials Engineering - TU-Dortmund, Leonhard-Euler-Str. 2, 44227 Dortmund, Germany) manuel.ferreira@udo.edu; J. Nellesen (RIF e.V. ─ Institut für Forschung und Transfer, Joseph-von-Fraunhofer-Str. 20, D 44227 Dortmund, Germany) jens.nellesen@rif-ev.de; M. Kansteiner (Institute of Machining Technology, TU Dortmund, Baroper Straße 303, 44227 Dortmund, Germany) kansteiner@isf.de; S. Herbrandt (Chair of Computational Statistics, TU-Dortmund, Technische Universität Dortmund - 44221 Dortmund, Germany) herbrandt@statistik.tu-dortmund.de

Abstract

Due to their outstanding wear resistance and hardness, diamond tools are mainly used for the machining of stone and concrete. These diamond cutting tools consist of small diamond grinding segments, which are fabricated powder-metallurgically. This production route combines a very ductile metallic binder component into which diamonds are embedded. Additionally, the sintering process of these composite materials offers a high degree of flexibility. The amount of diamonds, the grain size, and the metal matrix powder used can be fully adapted to the materials' characteristics of the machined concrete or stone. Although sintering and hot pressing are state of the art for the diamond tool production, the wear mechanisms on heterogeneous materials is difficult to evaluate with physical methods. Therefore, this paper focuses on a statistical method to investigate the influences of the diamond size, amount, and the computer tomographically calculated diamond distribution on machining parameters such as wear and forces.

Introduction

The natural stone industry and the demolition of concrete structures, especially reinforced concrete or the deconstruction of nuclear plants, have a high demand concerning abrasive machining tools, which must endure extremely high wear stresses during the grinding process on mineral materials. For these applications, diamond-metal composite materials are the best choice. These small diamond-containing grinding segments, attached to saw blades, drill bits or wire saws, are generally fabricated by a powder metallurgical process route [1]. This can be realized by conventional sintering processes, which have been established for decades in the diamond tool industry. Here the vacuum sintering and the hot pressing are the most important processes. The vacuum sintering process includes the pre-mixing of diamond-metal compounds (diamond amount 5-10 vol-%) and the densification by means of mechanical uniaxial pressing to obtain near-net-shape greenbodies. Because of the separation of two required process steps (pressing and sintering), the main disadvantages of vacuum sintering is on the one hand the resulting higher process time, and on the other hand a qualitatively worse materials characteristics due to pressure-less sintering. To avoid these issues and to realize a more productive fabrication process, the simultaneous pressing and sintering of diamond-metal composites has established itself [2,3,4,5]. Besides a conventional sintering of diamond tools, Tillmann et.al. investigated short-time sintering processes like FAST and CDS (Capacitor Discharge Sintering) which are made suitable for industrial diamond tool fabrication [6]. In addition to a better productivity by short time sintering of diamond segments, this technique inhibits diamond degrading effects, which results from the high temperatures during the sintering process. Detailed investigations regarding the chemical reactions at the diamond metal interface by means of XRD-phase analyses showed that the carbide formation and graphitization of diamonds is stronger in vacuum sintered samples because of the longer sintering time and higher temperature [7,8].

Due to the combination of a ductile metal binder with a hard and abrasive diamond grit, which is distributed into the metal matrix components, the machining mechanisms as well as the wear behaviour is well adapted for the removal of brittle mineral materials such as stone and concrete. Furthermore, the removal mechanisms during the machining of mineral materials strongly differ from the removal mechanisms of metals. The machining of brittle materials like concrete or stone shows a material removal which is not limited to the cutting edge (brittle fracture) [9,10]. This behaviour as well

as the high degree of heterogeneity in the diamond tools and mineral materials makes it difficult to describe the wear and removal mechanisms with physical evaluations. For this reason, statistical methods based on the design of experiments and regression models shall evaluate the dependencies between materials characteristics, machining parameters, and occurring forces. In addition, this paper focuses on the computertomographical investigation of both diamond wear and break-out as well as the influence on normal forces.

Experimental

Sample fabrication

An iron-based 4 component metal matrix powder (Diabase V21) was used for the single diamond segment production. The vol.-amount of diamonds and the grain size of the diamond was varied as shown in Table 1.

Table 1: Materials used

Sample	Diamond amount [vol-%]	Diamond size [us-mesh]	Diamond size [µm]
1.a	2	20/30	595-841
1.b	2	20/30	
1.c	5	20/30	
1.d	5	20/30	
1.e	10	20/30	
2.a	2	40/50	297-400
2.b	2	40/50	
2.c	5	40/50	
2.d	5	40/50	
2.e	10	40/50	
3.a	2	70/80	177-210
3.b	2	70/80	
3.c	5	70/80	
3.d	5	70/80	
3.e	10	70/80	

The prepared powder mixtures were hot pressed in a sintering facility of Dr. Fritsch in a graphite mould at a maximum temperature of 840°C with a holding time of 3 minutes. The compacted diamond-metal composite segments were brazed onto a screw for further machining tests (Fig. 1).

Fig. 1: Single segment sample

Machining tests

Table 2: Machining parameters

	Cutting speed v_c [m/min]	Feed rate v_f [mm/min]
1	155,25	2
2	40,5	1,25
3	155,25	1,25
4	270	1,25
5	155,25	0,5

The prepared single segment samples were attached in a Chiron FZ 12 S machining center on a rotating sample holder. Grinding tests were performed on concrete (C100) and reinforced concrete with the machining parameters given in Table 2. Normal forces (F_n) were permanently recorded by measuring boxes attached below the concrete block.

Computertomography

In order to analyze the spatial distribution of the diamonds the segments were imaged by micro tomography in the initial state, i.e. before the machining tests. The computertomographic measurements were carried out with a high-performance computertomography system which is equipped with a directional micro-focus tube and a large-sized flat panel-detector with an active area of 409.6 x 409.6 mm². For the 3D imaging of an entire segment which exhibits the following dimensions $\approx$ 10 mm $\times$ 5 mm $\times$ 8 mm radioscopic images of the segment were taken at 1000 rotational positions with an angle increment of 0.36 °. Each radioscopic image contained 1004 x 1024 binned square pixels. The segment was mapped with maximum magnification $m \approx 32$ onto the

detector plane which is given by the ratio of the distance between the focal spot and detector plane, i.e. 613 mm, and the distance between the focal spot and the rotation axis which was 19 mm. The acceleration voltage was set to 220 kV and a tube current of 60 µA was selected. The polychromatic radiation was prefiltered with a Cu sheet of 0.5 mm thickness. From the projections a tomogram consisting roughly of $900 \times 500 \times 700$ voxels was reconstructed using the well-known Feldkamp-algorithm [11]. The edge length of the cubic voxels was ≈12 µm.

Results

Statistical evaluation of force time series

Statistical evaluation and modelling was with "JMP". To determine the statistical dependencies of materials characteristics like diamond grain size and diamond volume amount, a regression model based on a 2nd degree polynomial was used. In the following two different regressions of samples which were used at cutting speeds of 270 respectively 40,5 m/min (v_f=1,25 mm/min) were presented.

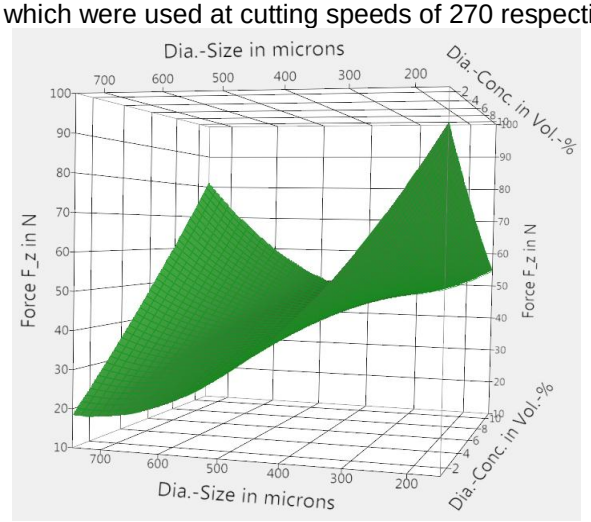

Fig. 2: Regression for Vc=270 m/min

Table 3: Regression parameters

	Estimate	t-value
intercept	61,044115	15,66
conc	0,7407888	1,64
size	-0,057662	-7,17
conc^2	0,0767976	0,40
conc*size	0,0167485	8,96
size^2	0,0002201	4,26
R^2=0,978		

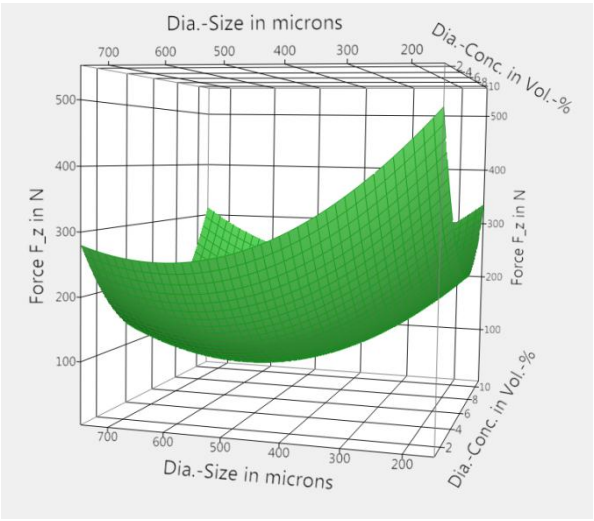

Fig. 3: Regression for Vc=40,5 m/min

Table 4: Regression parameters

	Estimate	t-value
intercept	263,74615	3,90
conc	-11,77615	-1,50
size	-0,271418	-1,95
conc^2	7,3706605	2,19
conc*size	0,0318785	0,98
size^2	0,0011011	1,23
R^2=0,768		

The two presented statistical evaluations show a difference in the material-dependent influences on occurring normal forces if the cutting speed is changed. Hereby the normal forces are strongly decreasing on tools with a low diamond amount and large grain size when using the maximal cutting speed (Fig.2). Nevertheless, both regressions tend to evaluate a decrease of normal forces using diamond tools with a diamond grain size and concentration in a medium range (400-500 µm; 5-6 vol-%). The maximum forces at both cutting speeds occur during the machining with tools which have on the one hand the highest amount and largest size of diamonds and on the other hand, have the smallest grain size and lowest concentration values.

Diamond break-out and force-time series

Supported by computertomography and reflected-light microscopy, in this chapter diamond breakout and diamond exposure has been shown. These visual illustrations of the wear and self-sharpening mechanisms of diamond segments, especially by before-later comparison, were finally related to the increasing respectively decreasing normal forces in force-time series.

A 3D tomogram which is reconstructed from the projections of a specimen approximates the spatial distribution of the linear attenuation coefficient μ_l, which is a function of the effective atomic number. In Fig. 4a) an xy-slice extracted from the 3D tomogram of sample 2.b is depicted. Since the linear attenuation coefficient is coded by grayscale it can be concluded that the diamonds are less attenuating than the cobalt matrix. The 3D polyhedral shape of the diamonds can be adumbrated in the 2D xy plane since the virtually cut diamonds show polygonal areas. Moreover, the inhomogeneity in the distribution of the diamonds within the segment can be grasped. The visualized xy slice (cf. Fig. 4a)) reveals the mean plane below the segment surface after the grinding-in process (cf. Fig. 8a). Thus, the sites of the diamonds and their arrangement in Fig. 4a) and Fig. 8a agree very well.

a) 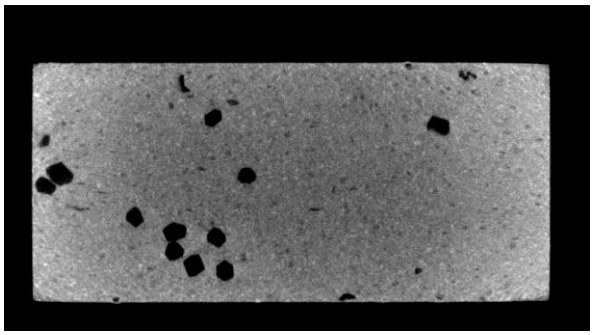 b) 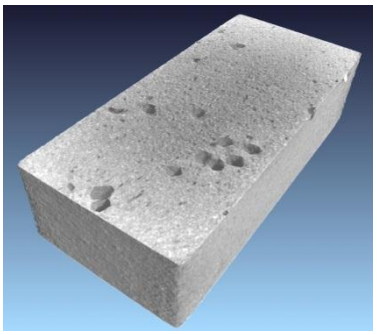

Fig. 4: a) 2D xz slice extracted from the 3D tomogram of sample 2.b which reveals the distribution of the dispersed diamonds (dark spots) in the cobalt matrix (bright surrounding area of the diamonds); b) volume-rendered representation of the plane shown in subfigure a)

In Fig. 5 the mean xy plane below the segment surface after the grinding-in of sample 3.d is rendered using the grayscale for the linear attenuation coefficient. Comparing the 2D slices in Fig. 4a) and Fig. 5 it is obvious that sample 2.b contains larger diamonds than specimen 3.d (cf. An iron-based 4 component metal matrix powder (Diabase V21) was used for the single diamond segment production. The vol.-amount of diamonds and the grain size of the diamond was varied as shown in Table 1.
Table 1). In Fig. 6 a photographic image of the surface (almost directly) after the grinding-in is visualized which corresponds to the 2D xy plane in Fig. 5 since the position of the diamonds agree very well. Furthermore, the 3D surface of specimen 3.d which is obtained by tomographic imaging of this specimen after the grinding-in process and which is volume-rendered in 6 (a) top view and b) arbitrary view) shows the same arrangement of the diamonds.

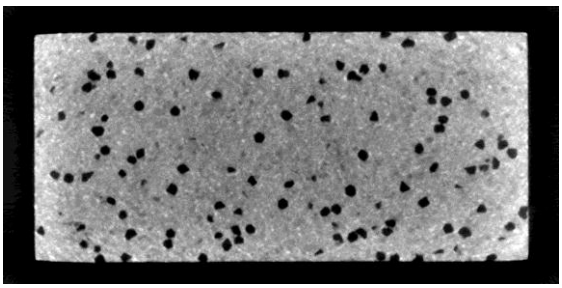

Fig. 5: 2D xz slice extracted from the 3D tomogram of sample 3.d which reveals the distribution of the dispersed diamonds (dark spots) in the cobalt matrix (bright surrounding area of the diamonds)

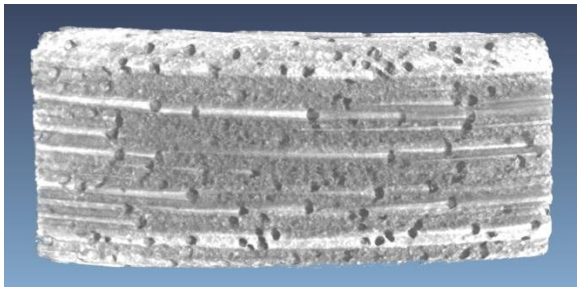

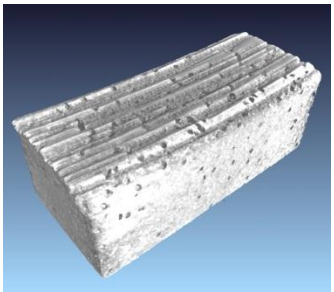

Fig. 6: volume-rendered 3D surface of specimen 3.d obtained by tomographic imaging after the grinding-in process a) top view, b) arbitrary view

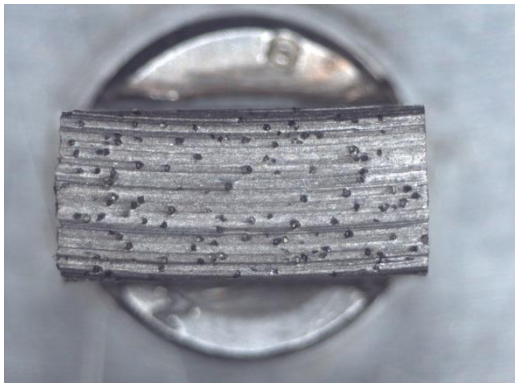

Fig. 7a: Sample 3.d - Test beginning

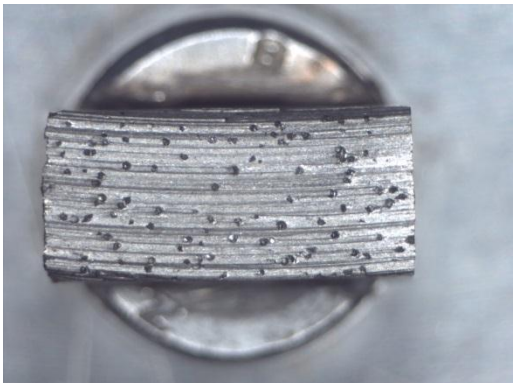

Fig.7b: Sample 3.d - Test ended

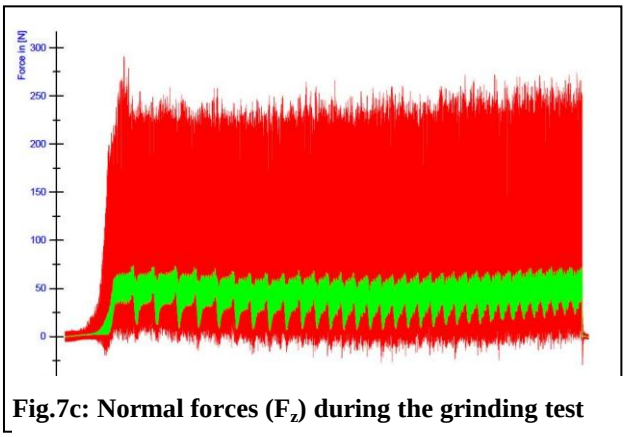

Fig.7c: Normal forces (F_z) during the grinding test

Fig. 7a-b show a sample without any definite change of the cutting edge. There is no visible diamond break-out or exposure during the machining process. Hence the force-time series is very regular and no abrupt increase or decrease of forces can be identified (Fig. 7c).

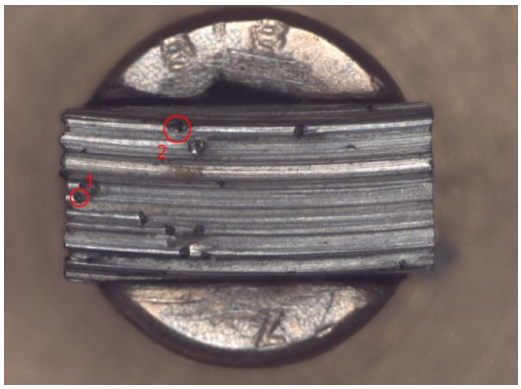

Fig.8a: Sample 2.b - Test beginning

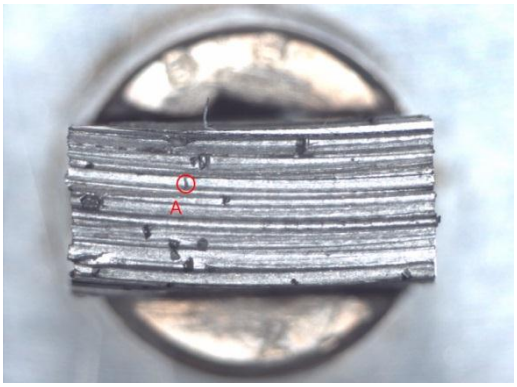

Fig.8b: Sample 2.b - Test ended

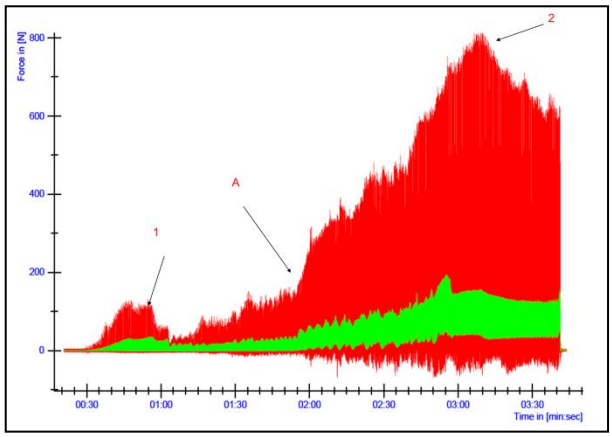

Fig.8c: Normal forces (Fz) during the grinding test

The measured forces during the machining of sample 2.b are much more irregular indicating

that the cutting edge is changing during the grinding process. Taking a closer look at microscope images and comparing the state before and after machining, two diamond break-outs can be identified at area 1 and 2 which results in a significant decrease of normal forces. Otherwise the diamond exposure at area A raises the normal forces shown in Fig.8c.

Conclusion

Both the influence of materials characteristics (concentration, size) and direct changes in the composition of the cutting edge during the machining process show significant influences on normal forces. The experiments showed that lowest forces are correlated with a diamond amount of 5-6 vol-% and a diamond size of 400µm-500µm.

Acknowledgements

This work is supported by the German Research Foundation (DFG) within the Research Centre SFB 823 TP B4.

References

[1] Denkena B., Tönshoff H. K., Friemuth T., Gierse A., Glatzel T., Hillmann-Apmann H.: Innovative Trennschleifprozesse in der Natursteinbearbeitung, Werkstatttechnik online, Jahrgang 92, H. 6, 2002, S. 290-296

[2] J. D. Dwan, “Production of diamond impregnated cutting tools”, Powder metallurgy, 1998, vol. 41, no. 2, pp. 84-86

[3] Konstanty J., Bunsch A.: Hot pressing of cobalt powders, Powder Metallurgy, Vol. 34, No. 3, 1991, S. 195-198

[4] B. Brook, „Principles of Diamond tool technology for sawing rock“, Int. J. of Rock Mechanics & Mining Sciences, 2002, vol.39, pp. 41-58

[5] W. Tillmann, M. Gathen, E. Vogli and C. Kronholz: Diamond Tool Production – Materials and Processing, PM Asia 2007 Conference & Exhibition, 2-4 April 2007, Shanghai, China,

[6] Tillmann, W., C. Kronholz, M. Ferreira, W. Theisen, A. Knote, P. Schütte and J. Schmidt: Comparison of Different Metal Matrix Systems for Diamond Tools Fabricated by New Current Induced Short-Time Sintering Processes. “Conference Proceedings Powder Metallurgy World Congress PM 2010”, Vol. 3, p. 531 – 538, 10. – 14. 10. 2010, Florenz/Italy

[7] A. Steffen, M. Ferreira, M. Paulus, W. Tillmann, and M. Tolan: Structure Analysis of the Interfacial Region between Diamonds and Metal Matrices, EuroPM2012 Proceedings, Vol. 2, p.125-130, 15: Diamond Tools + Ultrahard Materials

[8] Tillmann, W., Tolan, M., Ferreira, M., Thutewohl, S., Steffen, A.: Influence of hot pressing and vacuum sintering parameters on interfacial reactions in diamond-metal composites, EuroPM2013 Proceedings; Session 9: Diamond Tools

[9] G. J. Bullen, W. Brown: Verschleißverhalten von Diamantbohrkronen beim Einsatz auf Beton mit hochfester Stahlarmierung, Industrie Diamanten Rundschau, 18 (1984) 1, pp. 10–18

[10] B. Denkena, J. C. Becker, A. Gierse: Examination of Basic Separation Mechanisms for Machining Concrete and Stone. Production engineering, 2004, pp. 23–28

[11] Feldkamp, L. A.; Davis, L. C.; Kress, J. W.: Practical cone-beam algorithm. Journal of the Optical Society of America, 1 (1984) 6, pp. 612–619.